



Article

Involvement of MexS and MexEF-OprN in Resistance to Toxic Ion Chelators in *Pseudomonas putida* KT2440

Tania Henriquez ¹, Tom Baldow ¹, Yat Kei Lo ¹, Dina Weydert ¹, Andreas Brachmann ² and Heinrich Jung ^{1,*}

¹ Biozentrum, Mikrobiologie, Ludwig-Maximilians-Universität München, 82152 Martinsried, Germany; T.Henriquez@bio.lmu.de (T.H.); TomBaldow@gmx.de (T.B.); kei.lo@campus.lmu.de (Y.K.L.); Dina.Weydert@campus.lmu.de (D.W.)

² Biozentrum, Genetik, Ludwig-Maximilians-Universität München, 82152 Martinsried, Germany; brachmann@lmu.de

* Correspondence: hjung@lmu.de

Received: 23 October 2020; Accepted: 12 November 2020; Published: 14 November 2020



Abstract: Bacteria must be able to cope with harsh environments to survive. In Gram-negative bacteria like *Pseudomonas* species, resistance-nodulation-division (RND) transporters contribute to this task by pumping toxic compounds out of cells. Previously, we found that the RND system TtgABC of *Pseudomonas putida* KT2440 confers resistance to toxic metal chelators of the bipyridyl group. Here, we report that the incubation of a *ttgB* mutant in medium containing 2,2'-bipyridyl generated revertant strains able to grow in the presence of this compound. This trait was related to alterations in the *pp_2827* locus (homolog of *mexS* in *Pseudomonas aeruginosa*). The deletion and complementation of *pp_2827* confirmed the importance of the locus for the revertant phenotype. Furthermore, alteration in the *pp_2827* locus stimulated expression of the *mexEF-oprN* operon encoding an RND efflux pump. Deletion and complementation of *mexF* confirmed that the latter system can compensate the growth defect of the *ttgB* mutant in the presence of 2,2'-bipyridyl. To our knowledge, this is the first report on a role of *pp_2827* (*mexS*) in the regulation of *mexEF-oprN* in *P. putida* KT2440. The results expand the information about the significance of MexEF-OprN in the stress response of *P. putida* KT2440 and the mechanisms for coping with bipyridyl toxicity.

Keywords: *Pseudomonas*; second site revertant; RND transporter; bipyridyls

1. Introduction

Pseudomonas species are Gram-negative rod-shaped bacteria that exhibit a highly versatile range of activities, including acting as plant protectants (such as *Pseudomonas putida*) or animal pathogens (such as *Pseudomonas aeruginosa*) [1,2]. The bacteria live in changing environments in which they must adapt and respond to stress in order to survive. Resistance-nodulation-division (RND) transport systems contribute to this task by pumping toxic compounds out of cells [3,4]. For example, the expression of *mexXY* is elevated in the presence of ribosome-targeting antibiotics [5], while the *mexCD-oprJ* operon is induced by membrane damaging agents [6]. Furthermore, several clinical isolates of *P. aeruginosa* exhibit the so-called *nfxC* phenotype that is characterized by expression of the normally quiescent *mexEF-oprN* operon (conferring resistance to quinolones and chloramphenicol), and the downregulation of *oprD* (leading to a decreased uptake of imipenem [7]). The phenotype was originally described in *P. aeruginosa* strain PAO4009 after exposure to norfloxacin [8]. The mutation leading to this phenotype can be located in *mexT* (coding for a regulator of *mexEF-oprN* and *oprD*) [9], *mexS* (regulator of *mexT*) [9], *mexEF-oprN*, *oprD*, *mvaT* [10], *ampR* [11] (the latter two genes code for transcriptional regulators), or in other unknown regions of the genome [12,13]. While most of this information on MexEF-OprN and its

regulatory network was derived from clinical isolates of *P. aeruginosa*, little is known about the role and regulation of the RND system in other species, including *P. putida*.

In our previous work, we described that in *P. putida* KT2440 the RND system TtgABC is needed in order to cope with the toxicity of the metal chelating compounds 2,2'-bipyridyl (Bip) and caerulomycin (a 2,2'-bipyridyl-derivative produced by bacteria and normally found in the environment [14]) [15]. In the absence of a functional transporter, Bip is most likely accumulated inside the cells, where it can sequester copper, iron and other metals, thereby interrupting the normal functioning of metal-dependent enzymes and protein complexes. Indeed, we observed that a *ttgB* mutant (lacking the inner membrane component of the TtgABC system) had an impaired growth phenotype and showed several metabolic defects in the presence of Bip (such as reduced intracellular ATP levels and inhibition of siderophore production) [15].

In the present work, we report the generation and characterization of second site revertants of a *ttgB* mutant of *P. putida* KT2440. Revertants were isolated after prolonged incubation of the *ttgB* mutant in presence of Bip and were able to grow in the presence of this compound (like *P. putida* KT2440 wild type strain). The molecular determinants of the phenotype were identified and evaluated by deletion and complementation experiments as well as gene expression analyses. Our results indicate that expression of the genes encoding the RND system MexEF-OprN is responsible for restoring the resistance to Bip in the *ttgB* mutant revertants. Expression of *mexEF-oprN* was dependent on alterations in the *pp_2827* locus (*mexS*). The results obtained by these experiments provide insights into the role of MexEF-OprN in stress response and reveal components involved in its regulation in *P. putida* KT2440.

2. Materials and Methods

2.1. Bacterial Strains and Culture Media

A complete list of strains, plasmids, and oligonucleotides used in this research can be found in Table 1 and Table S1. The strains were cultured in King's Broth (KB) medium [16] at 30 °C and stored as frozen glycerol stocks. 2,2'-Bipyridyl (Bip) (Sigma) was added to the medium at final concentrations of 0.5 or 1 mM when appropriate. For experiments in *P. putida* using plasmids, 1 mg/mL ampicillin or 50 µg/mL kanamycin was used. For susceptibility testing, Mueller Hinton (MH) medium was prepared according to the manufacturer's instructions.

Table 1. List of strains and plasmids used in this study.

Name (Strains)	Description	Source
Wild type (WT)	<i>Pseudomonas putida</i> KT2440	[17]
$\Delta ttgB$	Derived from strain KT2440 by deletion of <i>pp_1385</i>	[15]
Revertant A, B and C	Spontaneous second site revertants of $\Delta ttgB$ strain	This work
$\Delta ttgB \Delta pp_2827$	Derived from the $\Delta ttgB$ strain by deletion of <i>pp_2827</i>	This work
Δpp_2827	Derived from strain KT2440 by deletion of <i>pp_2827</i>	This work
Revertant A $\Delta mexF$	Derived from Revertant A strain by deletion of <i>pp_3426</i>	This work
$\Delta ttgB \Delta pp_2827 \Delta mexF$	Derived from the $\Delta ttgB \Delta pp_2827$ strain by deletion of <i>pp_3426</i>	This work
Name (plasmid)	Description	Source
pUCP (pUCP-Nde)	pUCP-NdeI (Amp ^R) shuttle vector	[18]
pUCP- <i>ttgB</i>	Derived from pUCP by cloning the <i>ttgB</i> gene from wild type strain into the multicloning site	[15]
pUCP- <i>pp_2827</i>	Derived from pUCP by cloning <i>pp_2827</i> from wild type strain into the multicloning site	This work
pSEVA224	Km ^R ; pSEVA221 derivative with <i>lacI^q/P_{trc}</i> expression system	[19]
pSEVA224- <i>mexF</i>	pSEVA224 derivative with <i>pp_3426</i> cloned into the multicloning site	This work
pBBR1-MCS5- <i>lux</i>	pBBR1-based plasmid containing promoter-less <i>luxCDABE</i> , and the <i>aacC1</i> gene (Gen ^R)	[20]
pBBR1-MCS5- <i>P_{mexE}::lux</i>	pBBR1-MCS5- <i>lux</i> derivative containing <i>P_{mexE}::luxCDABE</i>	This work

2.2. Colony Morphology Assay

The original protocol from Sakhtah and colleagues [21] was slightly modified. Briefly, overnight cultures were adjusted to an OD₆₀₀ of 3. Then, 10 µL were spotted onto KB agar plates and KB plus 1 mM Bip and incubated at 30 °C for 24 h. The colonies were photographed under visible and UV light. The final image processing was done with ImageJ [22] and Adobe Illustrator.

2.3. Generation of Mutants and Complemented Strains

All genes were deleted by homologous recombination using the pNPTS138-R6KT suicide vector [23]. Briefly, upstream and downstream regions of the area to be deleted were amplified and fused by PCR. The resulting amplicon was cloned into pNPTS138-R6KT and used to transform the corresponding initial strain (first recombination). This strain was then grown on cetrimide agar plus 10% sucrose in order to select for the second recombination. The mutant strain was screened by PCR and confirmed by DNA sequencing. For complementation, pp₂₈₂₇ and *mexF* were amplified by PCR, cloned into the corresponding plasmid (pUCP-Nde and pSEVA224) and used to transform *P. putida* strains. All oligonucleotides used for amplification are listed in Table S1.

2.4. Growth Curves

Overnight cultures in KB medium were used to inoculate baffled flasks with 35 mL of KB or KB plus 0.5 mM Bip (initial OD₆₀₀ of ~0.1). The flasks were incubated at 30 °C with continuous shaking at 180 rpm for 8 h. Every 60 min, 1 mL of bacterial culture was taken and used to measure OD₆₀₀. Each experiment was performed a minimum of three times and the data shown in respective graphs represent the average of all replicates.

2.5. Luciferase Activity Assay

A *P_{mexF}::luxCDABE* transcriptional reporter gene fusion was generated by PCR amplification of the promoter region of the *mexEF-oprN* operon and cloning of the resulting fragment into the BamHI and XhoI sites of plasmid pBBR1-MSC5-*lux* [20]. *P. putida* strains were transformed with the resulting plasmid pBBR1-MCS5-*P_{mex}::lux*. Overnight cultures of the resulting strains were used to inoculate 96-well plate in KB with or without 0.5 mM Bip and 30 µg/mL gentamicin. The final volume of the wells was 100 µL with an initial OD₆₀₀ of 0.1. The experiment was performed at 30 °C with continuous shaking for 12 h. After 8 h of growth, luminescence was measured and normalized against the OD₆₀₀ of each strain. Growth and luminescence were measured in a CLARIOstar Plus (BMG LABTECH®, Ortenberg, Germany).

2.6. Susceptibility Testing by Diffusion Method

Bacteria were grown on MH agar plates and then used to prepare an inoculum on saline solution (0.85% w/v NaCl) equivalent to a McFarland 0.5 (OD₆₂₅ of 0.08–0.13). This bacterial suspension was used to inoculate a new MH plate with a cotton swab. The inoculation was made over the plate in three different directions (to get a complete lawn). Then, susceptibility discs from Thermo Scientific™ Oxoid™ were placed over the plate using an antimicrobial susceptibility disc dispenser (Thermo Scientific™ Oxoid™, Waltham, MA, USA) and pressed against the agar with tweezers. For this assay, discs of Gentamicin (10 µg) and chloramphenicol (30 µg) were used. Finally, the plates were incubated for 18 h at 30 °C and the inhibition zone around each antibiotic was measured with a ruler.

2.7. Genomic Sequence Analysis

Genomic DNA of revertant and wild type strains was extracted using the Wizard® SV Genomic DNA Purification System (Promega) and for each sample purity was determined on NanoDrop ND-1000 (PiqLab). Library preparation was performed with 100 ng of genomic DNA each, as quantified on Qubit 2.0 Fluorometer (ThermoFisher Scientific with ds HS Assay Kit), using the Nextera DNA Flex

Library Prep Kit (Illumina) according to manufacturer's instructions. Libraries were quality controlled with DNA High Sensitivity DNA Kit on Bioanalyzer (Agilent) and quantified on Qubit 2.0 Fluorometer (ThermoFisher Scientific with ds HS Assay Kit). Genome sequencing was performed in the Genomics Service Unit (LMU Biocenter, Munich, Germany) on Illumina MiSeq with v3 chemistry (2× 250 bp paired-end sequencing). Genome assemblies and variant detection were performed on CLC Genomics Workbench 9 (Qiagen). The data have been deposited with links to BioProject accession number PRJNA670853 in the NCBI BioProject database (<https://www.ncbi.nlm.nih.gov/bioproject/>).

2.8. Statistical Analysis

GraphPad/Prism 8 was used for statistical analysis. One-way ANOVA with Dunnett's multiple comparison and *t*-test were performed as appropriated. All experiments were performed a minimum of three times.

3. Results

3.1. Bip-Driven Generation of Second Site Revertant Strains from the *ttgB* Mutant

In our previous research, we have described that deletion of *ttgB* creates a growth defect in presence of Bip and inhibits the production of the siderophore pyoverdine [15]. This phenotype was most likely related to the accumulation of Bip inside the cell in absence of a functional TtgABC system. In the course of subsequent experiments, we observed that after prolonged incubation in presence of 1 mM Bip, the $\Delta ttgB$ strain derived from *P. putida* KT2440 started to grow. More specifically, in a colony morphology assay on KB agar plates supplemented with 1 mM Bip, *P. putida* KT2440 (wild type) formed a large colony, while the $\Delta ttgB$ mutant yielded very small colonies in the inoculated area within 24 h (Figure 1A). Furthermore, when exposed to UV light, wild type colonies and the small colonies derived from the $\Delta ttgB$ mutant were fluorescent, suggesting that the cells produced the siderophore pyoverdine under the indicated experimental conditions (Figure 1A). We wondered if the small colonies were the result of very slow growth of the mutant or due to compensating mutations elsewhere in the genome. In order to answer this question, bacteria of the small colonies were isolated on KB agar plates without Bip and the colony morphology assay was repeated. Contrary to the original $\Delta ttgB$ mutant, all isolates formed large colonies in the presence of Bip, similar to wild type. More quantitative analyses of the growth dynamics in liquid KB medium containing 1 mM Bip revealed that the growth of the isolated strains was faster compared to the $\Delta ttgB$ mutant and even similar to the wild type (Figure 1B). In the absence of Bip, wild type, original $\Delta ttgB$ mutant and isolated strains grew equally well in KB medium (Figure 1B). Altogether, these results suggest that (an) additional mutation(s) compensate(s) for the deletion of *ttgB* in the isolated strains (called hereafter Revertants A, B and C) and restored the resistance against Bip.

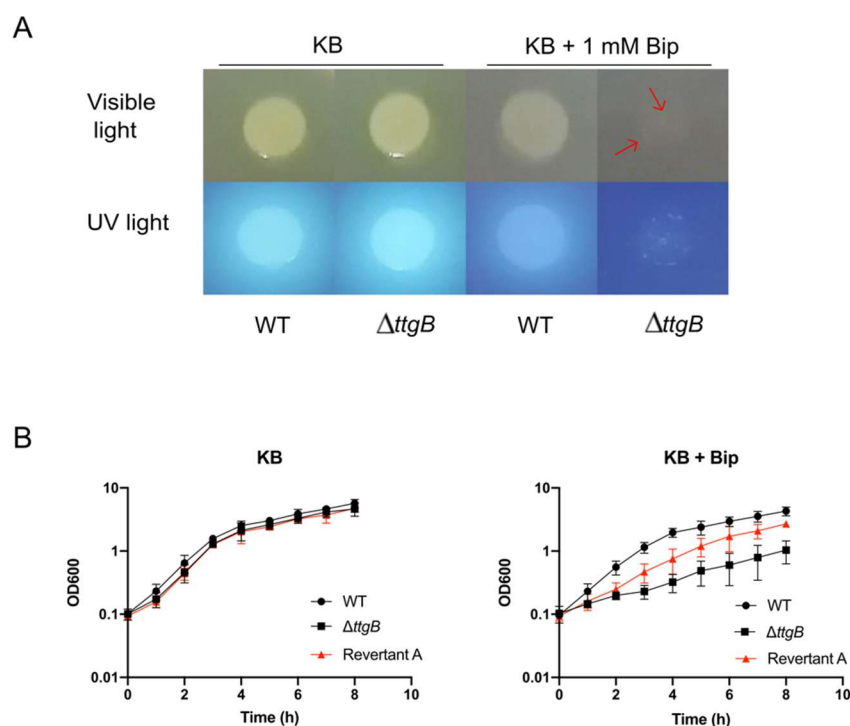


Figure 1. Second site mutation rescues growth of $\Delta ttgB$ strain in presence of Bip. **(A)** Overnight cultures were spotted onto King's Broth (KB) agar plates with or without supplementation with 1 mM Bip and incubated at 30 °C. After 24 h, pictures were taken using visible and UV light. The red arrows indicate the position of some of the revertant colonies that are better visible in UV light. **(B)** Growth curves of wild type, $\Delta ttgB$ and Revertant A strain (red) were performed in KB and KB plus 0.5 mM Bip for 8 h at 30 °C and continuous shaking (180 rpm). One ml of culture was taken and used to record its OD_{600} every 60 min. Experiments were performed a minimum of three times.

3.2. Alteration in *pp_2827* Rescues Growth of the *ttgB* Mutant in Presence of Bip

To obtain information on the molecular basis of the second site mutation in Revertants A, B and C, a genomic sequence analysis was performed. In Revertant A, a single base substitution was found in locus *pp_2827* (A841G), predicted to encode a 340 amino acid oxidoreductase/dehydrogenase [24,25]. The alteration would lead to the substitution of the amino acid isoleucine by valine (I281V) in the putative zinc-binding cassette of the predicted enzyme (Supplementary Material, Figure S1A). In Revertant B, we found an insertion of 17-kb-long transposon Tn4652 (Tsuda & Iino, 1987) after position 891 in *pp_2827*, leading to a replacement of the 43 C-terminal amino acids. This fusion also disrupts the putative zinc-binding cassette (Supplementary materials, Figure S1A). In Revertant C, a 250 kb genomic region between *pp_3382* and *pp_3585* is present in multiple copies (Supplementary Material, Figure S1B). This region is flanked by *pp_3381* and *pp_3586*, two copies of the IS110-like element ISPpu9, which is present 7 times in the *P. putida* KT2440 genome [26]. We focused on Revertant A in subsequent analyses.

To further investigate the role of *pp_2827* in the revertant phenotype, we deleted *pp_2827* in the $\Delta ttgB$ mutant. Our results indicated that the growth advantage of the $\Delta ttgB \Delta pp_2827$ strain in presence of Bip was similar to the Revertant A strain (Figure 2A). In parallel, deletion of *pp_2827* in the wild type strain did not result in any growth difference (Figure 2A). Obviously, the functional TtgABC system of the wild type was able to cope with Bip toxicity. In accordance with these results, the complementation of *pp_2827* in the $\Delta ttgB \Delta pp_2827$ strain made the bacterium susceptible to the toxicity of Bip (Figure 2B). Taken together, these results indicate that alterations in the locus *pp_2827* can rescue growth of the *ttgB* mutant in presence of Bip.

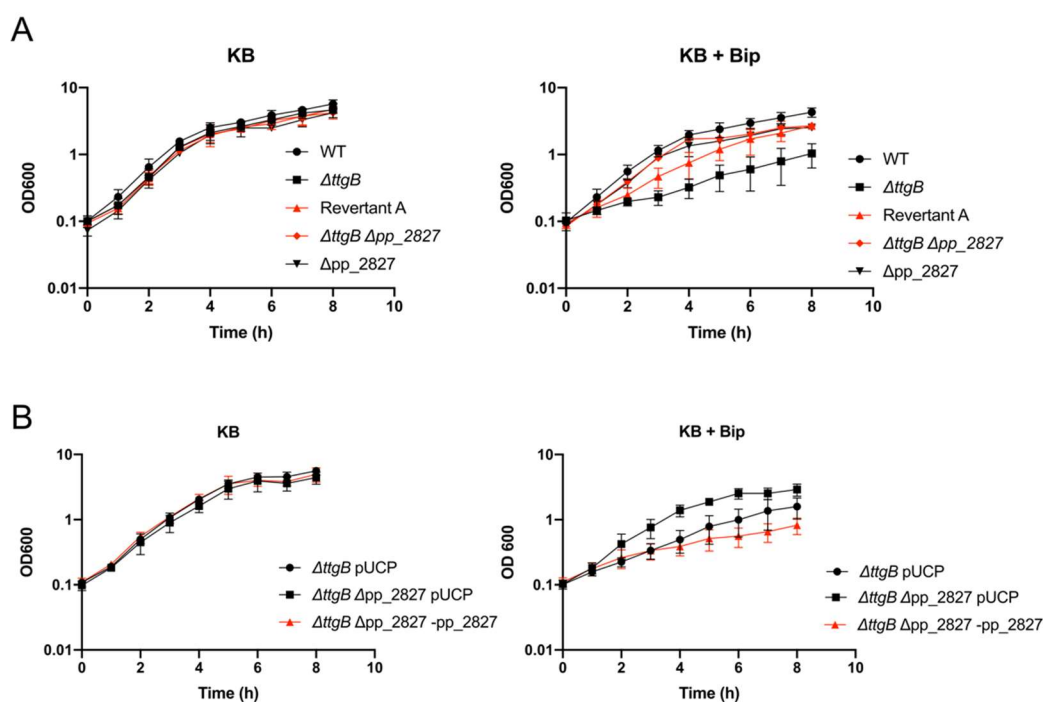


Figure 2. Alteration in the locus *pp_2827* affects growth of the $\Delta ttgB$ mutant in presence of Bip. (A) Growth curve of wild type, $\Delta ttgB$, Δpp_{2827} and strains with revertant phenotype (in red: Revertant A and the engineered $\Delta ttgB \Delta pp_{2827}$ strain). (B) Expression of *pp_2827* from plasmid pUCP-*pp_2827* reduces growth of the $\Delta ttgB \Delta pp_{2827}$ strain. For (A,B), growth curves were recorded in KB and KB plus 0.5 mM Bip at 30 °C and continuous shaking (180 rpm) for 8 h. Every 60 min, 1 mL of culture was taken and used to measure the OD₆₀₀. Experiments were performed a minimum of three times.

3.3. Alterations in *pp_2827* Confer Bip Resistance by Stimulating Expression of *mexEF-oprN*

In order to further explore the resistance mechanism to Bip in Revertant A, we analyzed possible links of *pp_2827* to other genes. In *P. aeruginosa*, the locus orthologous to *pp_2827* is *pa2491* (*mexS*), which together with the regulator gene *pa2492* (*mexT*) is located immediately upstream of the *mexEF-oprN* operon (*pa2493*–*pa2495*) [27]. The gene products of both *mexS* and *mexT* were previously implicated in the regulation of the expression of *mexEF-oprN* [9,28,29], an RND transporter that is normally quiescent in *P. aeruginosa* [30]. In *P. putida* KT2440, *pp_2827* and *pp_2826* (*mexT*), and the loci orthologous to *mexEF-oprN* (*pp_3425*–*pp_3427*) are located far away from each other in the genome [24,25]. The role of *pp_2827* in *P. putida*, to our knowledge, has not been explored yet.

Thus, we wondered if the observed phenotype in the revertant strains was due to *pp_2827* mutation influencing the activity of the MexEF-OprN efflux system. To that end, we analyzed the expression of *mexEF-oprN* in these strains through a transcriptional fusion that contained the promoter of *mexE* fused to the *luxCDABE* operon ($P_{mexE}::luxCDABE$) in plasmid pBBR1-MS5-*lux*. Our results showed that after 8 h of growth, the relative luminescence (normalized against OD₆₀₀) of the Revertant A strain was much higher than the one from the wild type strain (Figure 3), indicating that the *mexEF-oprN* promoter was active.

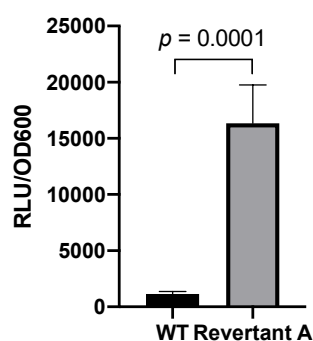


Figure 3. Promoter activity of the *mexEF-oprN* operon in *P. putida* KT2440 in presence of Bip. The transcriptional gene fusion using the *lux* reporter was generated by cloning the promoter region of *mexEF-oprN* into the BBR1-MCS5-*lux* plasmid. For the luciferase assay, overnight cultures of the transformed strains were grown in KB in presence of 0.5 mM Bip and 30 μ g/mL gentamicin. After 8 h of growth, the relative light units (RLU) were normalized against the OD₆₀₀ of the cultures. Experiments were performed a minimum of three times.

Additionally, the activity of the MexEF-OprN system was indirectly observed through an increased resistance of Revertant A strain to chloramphenicol, while there was no effect in the susceptibility to gentamicin (Figure 4). These results fit to the previously observed MexEF-OprN-mediated resistance pattern of *P. aeruginosa* [31].

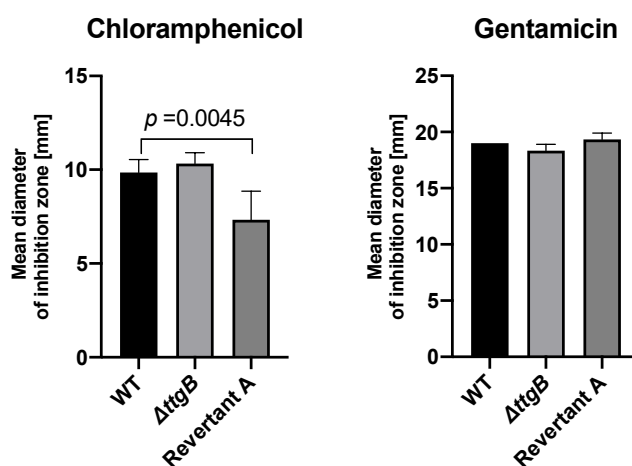


Figure 4. Susceptibility of the Revertant A strain to chloramphenicol. Susceptibility of wild type Δ ttgB and Revertant A strains was tested against chloramphenicol in Mueller Hinton (MH) medium through disc diffusion method. Plates were incubated at 30 °C for 18 h, and the halo diameter was measured. Experiments were performed a minimum of three times.

In *P. aeruginosa*, the impairment of *mexS*, and the concomitant activation of *mexT*, increases the expression not only of *mexEF-oprN* but also affects other genes (e.g., it represses *oprD*) [32]. Therefore, we wondered whether the Revertant A phenotype in *P. putida* was indeed due to the enhanced expression of the RND system or due to another element regulated by this network. Thus, we deleted the inner membrane component of the RND system, *mexF*, in the Δ ttgB Δ pp_2827 strain and in Revertant A. Our results showed that both strains lost the resistance to Bip when *mexF* was deleted (Figure 5). On the contrary, in the absence of Bip all strains grew equally well (Figure 5). This indicates that a functional MexEF-OprN system is required for the phenotype of Revertant A. These results were corroborated by complementation experiments, where the expression of *mexF* from a plasmid was able to rescue the growth of the strains similarly as the plasmid-based expression of *ttgB* (Supplementary

Materials, Figure S2). Altogether the results indicate that in Revertant A enhanced expression of *mexEF-oprN* is necessary to cope with Bip toxicity in the absence of a functional TtgABC.

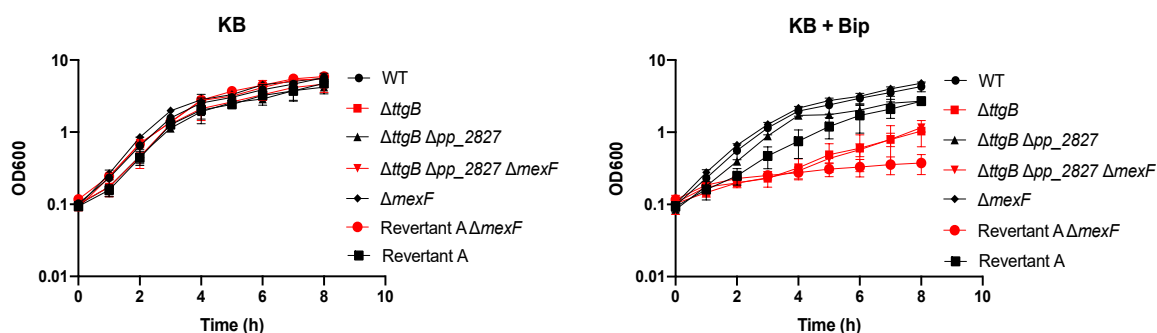


Figure 5. Growth of $\Delta ttgB$ -derivative strains in presence of Bip is due to MexEF-OprN activity. Bacterial growth was analyzed through growth curves in KB medium supplemented with 0.5 mM Bip at 30 °C with continuous shaking (180 rpm). To that end, overnight cultures were used to inoculate 35 mL of medium (initial OD₆₀₀ of 0.1). Every 60 min, OD₆₀₀ was measured. Strains with phenotype similar to the original $\Delta ttgB$ strain ($\Delta ttgB \Delta pp_2827 \Delta mexF$ and Revertant A $\Delta mexF$) are shown in red. Data are presented as an average of three independent experiments.

3.4. The *mexEF-oprN* Operon is also Upregulated in Revertants B and C

To obtain more information on the molecular basis of Bip resistance in the other revertant strains, we analyzed expression of the *mexEF-oprN* operon also in Revertant B and C and the engineered $\Delta ttgB \Delta pp_2827$ strain using plasmid pBBR1-MCS5-*P_{mex}::lux*. Bioluminescence measurements revealed that all three strains expressed *mexEF-oprN*, although to different degrees (Figure 6). The higher expression of *mexEF-oprN* in the Revertant B can also be seen indirectly through the increase in the resistance to chloramphenicol (Figure S3). For Revertant B, upregulation of *mexEF-oprN* was expected since in the strain *pp_2827* was altered (transposon insertion) similar to what was observed for Revertant A (point mutation in *pp_2827*). However, the level of upregulation of the operon was about 20fold higher than in Revertant A and at about the same level as for the engineered $\Delta ttgB \Delta pp_2827$ strain (Figure 6). The mechanism for the moderate upregulation of the *mexEF-oprN* operon in Revertant C remained enigmatic.

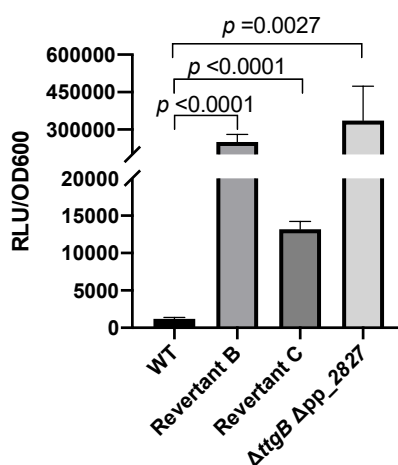


Figure 6. Promoter activity of the *mexEF-oprN* operon in *P. putida* KT2440 in presence of Bip. Overnight cultures of the strains containing the transcriptional fusion of the promoter of *mexEF-oprN* and the *luxCDABE* operon (in plasmid pBBR1-MCS5-*lux*) were grown in KB in presence of 0.5 mM Bip and 30 μ g/mL gentamicin. After 8 h, relative light units (RLU) were normalized against the OD₆₀₀. Data are presented as an average of at least three biological replicates.

4. Discussion

While inactivation of the RND system TtgABC renders *P. putida* KT2440 sensitive to metal ion chelators of the bipyridyl group [15], we describe here that incubation of a *ttgB* mutant of *P. putida* KT2440 in presence of Bip rapidly leads to the generation of second site revertant strains. Since intracellularly accumulated Bip interferes with the cellular homeostasis for iron, copper and potentially other metal ions required for central metabolic pathways and the respiratory chain, a rapid cellular response compensating the loss of TtgABC activity is not surprising. Known responses to intracellular metal ion limitation in bacteria include the stimulation of the uptake of metal ions, mobilization of limited metal ions from intracellular storage pools, and substitution of metal-dependent enzymes and pathways that function independently of the respective metal ion [33]. None of these possibilities seem to be used by *P. putida* KT2440 under our test conditions. Instead, the primary cause of intracellular ion limitation, the chelator Bip, seems to be removed from cells via an alternative RND system, MexEF-OprN. The latter system is known to be quiescent in *P. aeruginosa* [30], and we showed that the respective operon is also not expressed in *P. putida* KT2440, independent of the presence of Bip in the culture medium. However, in all three revertants generated from the *ttgB* mutant and analyzed here, *mexEF-oprN* was expressed constitutively. Deletion of *mexF* and plasmid-based complementation confirmed that the RND system is indeed required and most likely sufficient for rescuing growth of the $\Delta ttgB$ strain in the presence of Bip.

Identification of a point mutation and transposon insertion in the locus pp_2827 in the isolated Revertant A and B strains, respectively, and subsequent deletion and complementation analyses with pp_2827 demonstrate that PP_2827 represses the transcription of the *mexEF-oprN* operon. The gene product has been annotated as a zinc-dependent oxidoreductase/alcohol dehydrogenase in the genome of *P. putida* [24,25]. In a previous report, pp_2827 and *mexEF-oprN* were identified as belonging to the PhhR regulon that is made responsible for the activation of genes essential for phenylalanine degradation, phenylalanine homeostasis and other genes of unknown function [34]. However, to the best of our knowledge, this is the first report of an involvement of pp_2827 in the regulation of *mexEF-oprN* expression in *P. putida*. The locus adjacent to pp_2827, pp_2826, encodes a LysR-type transcriptional regulator termed MexT that was previously shown to stimulate *mexEF-oprN* expression in *P. putida* KT2440 [34]. Taken together, the results suggest a regulatory cascade, in which pp_2827 (MexS) inhibits the expression of the *mexEF-oprN* operon by repressing *mexT*. The mechanism of the repression is not known. The putative oxidoreductase MexS is not predicted to contain a DNA binding domain. So far, it can only be speculated that the enzyme produces a metabolite, alters the redox state of another compound or protein, or physically interacts with other proteins leading to repression of *mexT*. In this context, the relatively low levels of *mexEF-oprN* expression observed for Revertant A relative to Revertant B and the engineered $\Delta ttgB\Delta pp_2827$ strain may be due to an only partial inactivation of the putative oxidoreductase (MexS) in Revertant A, while in the latter two strains the enzyme is completely inactive. In fact, the point mutation in Revertant A causes an amino acid substitution (I281V) in the predicted zinc binding domain of the enzyme that may alter enzyme kinetics without abolishing activity. This is the first report showing that an alteration at this site can stimulate *mexEF-oprN* expression. In clinical isolates and laboratory generated spontaneous mutants of *P. aeruginosa* with elevated expression of *mexEF-oprN*, positions such as the N-terminal or the zinc-binding domain were altered in MexS [29,35]. While MexS-dependent regulation of *mexEF-oprN* is dependent of MexT in *P. aeruginosa* [29], another publication reports that MexS can in principal also have inhibitory effects on gene expression independently of MexT [36].

The molecular mechanisms behind the upregulation of *mexEF-oprN* in Revertant C may be due to transposon-based gene duplication events. Our genome comparisons do not hint at changes in the regions of *mexS*, *mexT*, *mexEF-oprN*, *mvaT*, *ampR*, which have been reported to be causative for the *nfxC* phenotype of *P. aeruginosa* [9–11]. This result is in accordance with previous reports in clinical strains of *P. aeruginosa*, where significant percentages of the screened strains had a *nfxC* phenotype with unknown mechanisms for the induction of *mexEF-oprN* expression [12]. Furthermore, the relatively

low level of expression of *mexEF-oprN* in Revertant C may be explained by a functional *pp_2827* (MexS) that most likely inhibits upregulation of the operon. Furthermore, for Revertant C it is not clear whether this upregulation is indeed responsible for Bip resistance. Although the large amplified genomic region (*pp_3382* and *pp_3585*) contains also the *mexEF-oprN* operon, an involvement of other molecular players cannot be excluded.

All three revertant strains analyzed here exhibit a behavior similar to the *nfxC* phenotype of *P. aeruginosa* [12,37], including the expression of *mexEF-oprN* and a higher resistance to chloramphenicol. In the native environment of the soil bacterium *P. putida* KT2440, MexEF-OprN could be involved in the detoxification of natural bipyridyls such as caeruleomycin and collismycin that are produced by other bacteria [14,38].

It is interesting to note how quickly (in less than 24 h of exposure) incubation in presence of Bip transformed the *ttgB* mutant into a much more resistant strain (increased resistance to Bip, chloramphenicol and probably other bipyridyls) by second site mutation. Two of the three revertants most likely stem from transposon activity, which at least for Tn4652 is known to be induced in *P. putida* under stress conditions [39]. From a clinical point of view, this reinforces the necessity to discover effective inhibitors of RND efflux pumps to avoid the fast appearance of spontaneous resistance. Altogether, these results increase the information about the role of MexEF-OprN in stress response in *P. putida* KT2440 and extend the role of MexS in *Pseudomonas* species.

Supplementary Materials: The following are available online at <http://www.mdpi.com/2076-2607/8/11/1782/s1>, Figure S1: Mutations in Revertant A, B and C strains, Figure S2: Phenotype complementation with *ttgB* and *mexF* in the Revertant A $\Delta mexF$ and $\Delta ttgB \Delta pp_2827 \Delta mexF$ strains, Figure S3: Susceptibility of Revertant B to chloramphenicol, Table S1: List of primers used in this study.

Author Contributions: Conceptualization, T.H. and H.J.; methodology, T.H. and H.J.; software, A.B., T.H., T.B., Y.K.L., D.W. and H.J.; validation, H.J. and T.H.; formal analysis, A.B., T.H., T.B., Y.K.L., D.W. and H.J.; investigation, T.H., T.B., Y.K.L., and D.W.; resources, H.J., A.B. and T.H.; data curation, H.J., A.B. and T.H.; writing—original draft preparation, H.J. and T.H.; writing—review and editing, H.J., A.B. and T.H.; visualization, H.J., A.B. and T.H.; supervision, H.J. and T.H.; project administration, H.J.; funding acquisition, H.J. All authors have read and agreed to the published version of the manuscript.

Funding: This research and the APC were funded by the Deutsche Forschungsgemeinschaft through grants JU333/5-1, 2 (SPP1617) and JU333/6-1.

Acknowledgments: We thank Michelle Eder for excellent technical assistance.

Conflicts of Interest: The authors declare no conflict of interest. The funders had no role in the design of the study; in the collection, analyses, or interpretation of data; in the writing of the manuscript, or in the decision to publish the results.

References

1. Timmis, K.N. *Pseudomonas putida*: A cosmopolitan opportunist par excellence. *Environ. Microbiol.* **2002**, *4*, 779–781. [[CrossRef](#)] [[PubMed](#)]
2. Palleroni, N.J. *Pseudomonas*. In *Bergey's Manual of Systematics of Archaea and Bacteria*; Wiley: Hoboken, NJ, USA, 2015. [[CrossRef](#)]
3. Dreier, J.; Ruggerone, P. Interaction of antibacterial compounds with RND efflux pumps in *Pseudomonas aeruginosa*. *Front. Microbiol.* **2015**, *6*. [[CrossRef](#)] [[PubMed](#)]
4. Poole, K. Stress responses as determinants of antimicrobial resistance in *Pseudomonas aeruginosa*: Multidrug efflux and more. *Can. J. Microbiol.* **2014**, *60*, 783–791. [[CrossRef](#)] [[PubMed](#)]
5. Morita, Y.; Sobel, M.L.; Poole, K. Antibiotic inducibility of the MexXY multidrug efflux system of *Pseudomonas aeruginosa*: Involvement of the antibiotic-inducible PA5471 gene product. *J. Bacteriol.* **2006**, *188*, 1847–1855. [[CrossRef](#)]
6. Fraud, S.; Campigotto, A.J.; Chen, Z.; Poole, K. MexCD-OprJ multidrug efflux system of *Pseudomonas aeruginosa*: Involvement in chlorhexidine resistance and induction by membrane-damaging agents dependent upon the AlgU stress response sigma factor. *Antimicrob. Agents Chemother.* **2008**, *52*, 4478–4482. [[CrossRef](#)]

7. Köhler, T.; van Delden, C.; Curty, L.K.; Hamzehpour, M.M.; Pechere, J.C. Overexpression of the MexEF-OprN multidrug efflux system affects cell-to-cell signaling in *Pseudomonas aeruginosa*. *J. Bacteriol.* **2001**, *183*, 5213–5222. [[CrossRef](#)]
8. Fukuda, H.; Hosaka, M.; Hirai, K.; Iyobe, S. New norfloxacin resistance gene in *Pseudomonas aeruginosa* PAO. *Antimicrob. Agents Chemother.* **1990**, *34*, 1757–1761. [[CrossRef](#)]
9. Fargier, E.; Mac Aogáin, M.; Mooij, M.J.; Woods, D.F.; Morrissey, J.P.; Dobson, A.D.; Adams, C.; O’Gara, F. MexT functions as a redox-responsive regulator modulating disulfide stress resistance in *Pseudomonas aeruginosa*. *J. Bacteriol.* **2012**, *194*, 3502–3511. [[CrossRef](#)]
10. Westfall, L.W.; Carty, N.L.; Layland, N.; Kuan, P.; Colmer-Hamood, J.A.; Hamood, A.N. *mvaT* mutation modifies the expression of the *Pseudomonas aeruginosa* multidrug efflux operon *mexEF-oprN*. *FEMS Microbiol. Lett.* **2006**, *255*, 247–254. [[CrossRef](#)]
11. Balasubramanian, D.; Schnepfer, L.; Merighi, M.; Smith, R.; Narasimhan, G.; Lory, S.; Mathee, K. The regulatory repertoire of *Pseudomonas aeruginosa* AmpC β -lactamase regulator AmpR includes virulence genes. *PLoS ONE* **2012**, *7*, e34067. [[CrossRef](#)]
12. Richardot, C.; Juarez, P.; Jeannot, K.; Patry, I.; Plésiat, P.; Llanes, C. Amino acid substitutions account for most MexS alterations in clinical *nfxC* mutants of *Pseudomonas aeruginosa*. *Antimicrob. Agents Chemother.* **2016**, *60*, 2302–2310. [[CrossRef](#)] [[PubMed](#)]
13. Zaoui, C.; Overhage, J.; Löns, D.; Zimmermann, A.; Müsken, M.; Bielecki, P.; Pustelny, C.; Becker, T.; Nimtz, M.; Häussler, S. An orphan sensor kinase controls quinolone signal production via MexT in *Pseudomonas aeruginosa*. *Mol. Microbiol.* **2012**, *83*, 536–547. [[CrossRef](#)] [[PubMed](#)]
14. Funk, A.; Divekar, P.V. Caerulomycin, a new antibiotic from *Streptomyces caerulescens* Baldacci. I. Production, isolation, assay, and biological properties. *Can. J. Microbiol.* **1959**, *5*, 317–321. [[CrossRef](#)] [[PubMed](#)]
15. Henríquez, T.; Stein, N.V.; Jung, H. Resistance to Bipyridyls Mediated by the TtgABC Efflux System in *Pseudomonas putida* KT2440. *Front. Microbiol.* **2020**, *11*. [[CrossRef](#)]
16. King, E.O.; Ward, M.K.; Raney, D.E. Two simple media for the demonstration of pyocyanin and fluorescein. *J. Lab. Clin. Med.* **1954**, *44*, 301–307. [[CrossRef](#)] [[PubMed](#)]
17. Bagdasarian, M.; Lurz, R.; Rückert, B.; Franklin, F.C.H.; Bagdasarian, M.M.; Frey, J.; Timmis, K.N. Specific-purpose plasmid cloning vectors II. Broad host range, high copy number, RSF 1010-derived vectors, and a host-vector system for gene cloning in *Pseudomonas*. *Gene* **1981**, *16*, 237–247. [[CrossRef](#)]
18. Cronin, C.N.; McIntire, W.S. pUCP-Nco and pUCP-Nde: *Escherichia-Pseudomonas* shuttle vectors for recombinant protein expression in *Pseudomonas*. *Anal. Biochem.* **1999**, *272*, 112–115. [[CrossRef](#)]
19. Silva-Rocha, R.; Martinez-Garcia, E.; Calles, B.; Chavarria, M.; Arce-Rodriguez, A.; de Las Heras, A.; Paez-Espino, A.D.; Durante-Rodriguez, G.; Kim, J.; Nickel, P.I.; et al. The Standard European Vector Architecture (SEVA): A coherent platform for the analysis and deployment of complex prokaryotic phenotypes. *Nucleic Acids Res.* **2013**, *41*, D666–D675. [[CrossRef](#)]
20. Gödeke, J.; Heun, M.; Bubendorfer, S.; Paul, K.; Thormann, K.M. Roles of two *Shewanella oneidensis* MR-1 extracellular endonucleases. *Appl. Environ. Microbiol.* **2011**, *77*, 5342–5351. [[CrossRef](#)]
21. Sakhtah, H.; Koyama, L.; Zhang, Y.; Morales, D.K.; Fields, B.L.; Price-Whelan, A.; Hogan, D.A.; Shepard, K.; Dietrich, L.E.P. The *Pseudomonas aeruginosa* efflux pump MexGHI-OpmD transports a natural phenazine that controls gene expression and biofilm development. *Proc. Natl. Acad. Sci. USA* **2016**, *113*, E3538–E3547. [[CrossRef](#)]
22. Schindelin, J.; Arganda-Carreras, I.; Frise, E.; Kaynig, V.; Longair, M.; Pietzsch, T.; Preibisch, S.; Rueden, C.; Saalfeld, S.; Schmid, B.; et al. Fiji: An open-source platform for biological-image analysis. *Nat. Methods* **2012**, *9*, 676–682. [[CrossRef](#)] [[PubMed](#)]
23. Lassak, J.; Henche, A.-L.; Binnenkade, L.; Thormann, K.M. ArcS, the cognate sensor kinase in an atypical Arc system of *Shewanella oneidensis* MR-1. *Appl. Environ. Microbiol.* **2010**, *76*, 3263–3274. [[CrossRef](#)] [[PubMed](#)]
24. Winsor, G.L.; Griffiths, E.J.; Lo, R.; Dhillon, B.K.; Shay, J.A.; Brinkman, F.S. Enhanced annotations and features for comparing thousands of *Pseudomonas* genomes in the *Pseudomonas* genome database. *Nucleic Acids Res.* **2016**, *44*, D646–D653. [[CrossRef](#)] [[PubMed](#)]
25. Nelson, K.E.; Weinel, C.; Paulsen, I.T.; Dodson, R.J.; Hilbert, H.; Martins dos Santos, V.A.; Fouts, D.E.; Gill, S.R.; Pop, M.; Holmes, M.; et al. Complete genome sequence and comparative analysis of the metabolically versatile *Pseudomonas putida* KT2440. *Environ. Microbiol.* **2002**, *4*, 799–808. [[CrossRef](#)]

26. Wu, X.; Monchy, S.; Taghavi, S.; Zhu, W.; Ramos, J.; van der Lelie, D. Comparative genomics and functional analysis of niche-specific adaptation in *Pseudomonas Putida*. *FEMS Microbiol. Rev.* **2011**, *35*, 299–323. [[CrossRef](#)]
27. Stover, C.K.; Pham, X.Q.; Erwin, A.L.; Mizoguchi, S.D.; Warrenner, P.; Hickey, M.J.; Brinkman, F.S.; Hufnagle, W.O.; Kowalik, D.J.; Lagrou, M.; et al. Complete genome sequence of *Pseudomonas aeruginosa* PAO1, an opportunistic pathogen. *Nature* **2000**, *406*, 959–964. [[CrossRef](#)]
28. Jin, Y.; Yang, H.; Qiao, M.; Jin, S. MexT regulates the type III secretion system through MexS and PtrC in *Pseudomonas aeruginosa*. *J. Bacteriol.* **2011**, *193*, 399–410. [[CrossRef](#)]
29. Sobel, M.L.; Neshat, S.; Poole, K. Mutations in PA2491 (*mexS*) promote MexT-dependent *mexEF-oprN* expression and multidrug resistance in a clinical strain of *Pseudomonas aeruginosa*. *J. Bacteriol.* **2005**, *187*, 1246–1253. [[CrossRef](#)]
30. Köhler, T.; Michéa-Hamzehpour, M.; Henze, U.; Gotoh, N.; Curty, L.K.; Pechère, J.C. Characterization of MexE-MexF-OprN, a positively regulated multidrug efflux system of *Pseudomonas aeruginosa*. *Mol. Microbiol.* **1997**, *23*, 345–354. [[CrossRef](#)]
31. Fetar, H.; Gilmour, C.; Klinoski, R.; Daigle, D.M.; Dean, C.R.; Poole, K. *mexEF-oprN* multidrug efflux operon of *Pseudomonas aeruginosa*: Regulation by the MexT activator in response to nitrosative stress and chloramphenicol. *Antimicrob. Agents Chemother.* **2011**, *55*, 508–514. [[CrossRef](#)]
32. Köhler, T.; Epp, S.F.; Curty, L.K.; Pechère, J.C. Characterization of MexT, the regulator of the MexE-MexF-OprN multidrug efflux system of *Pseudomonas aeruginosa*. *J. Bacteriol.* **1999**, *181*, 6300–6305. [[CrossRef](#)] [[PubMed](#)]
33. Chandrangsu, P.; Rensing, C.; Helmman, J.D. Metal homeostasis and resistance in bacteria. *Nat. Rev. Microbiol.* **2017**, *15*, 338–350. [[CrossRef](#)] [[PubMed](#)]
34. Herrera, M.C.; Duque, E.; Rodríguez-Herva, J.J.; Fernández-Escamilla, A.M.; Ramos, J.L. Identification and characterization of the PhhR regulon in *Pseudomonas putida*. *Environ. Microbiol.* **2010**, *12*, 1427–1438. [[CrossRef](#)] [[PubMed](#)]
35. Morita, Y.; Tomida, J.; Kawamura, Y. Efflux-mediated fluoroquinolone resistance in the multidrug-resistant *Pseudomonas aeruginosa* clinical isolate PA7: Identification of a novel MexS variant involved in upregulation of the *mexEF-oprN* multidrug efflux operon. *Front. Microbiol.* **2015**, *6*. [[CrossRef](#)] [[PubMed](#)]
36. Uwate, M.; Ichise, Y.K.; Shirai, A.; Omasa, T.; Nakae, T.; Maseda, H. Two routes of MexS-MexT-mediated regulation of MexEF-OprN and MexAB-OprM efflux pump expression in *Pseudomonas aeruginosa*. *Microbiol. Immunol.* **2013**, *57*, 263–272. [[CrossRef](#)] [[PubMed](#)]
37. Mooij, M.J.; O'Connor, H.F.; Tian, Z.X.; Wang, Y.P.; Adams, C.; Morrissey, J.P.; O'Gara, F. Antibiotic selection leads to inadvertent selection of *nfxC*-type phenotypic mutants in *Pseudomonas aeruginosa*. *Environ. Microbiol. Rep.* **2010**, *2*, 461–464. [[CrossRef](#)] [[PubMed](#)]
38. Gomi, S.; Amano, S.; Sato, E.; Miyadoh, S.; Kodama, Y. Novel antibiotics SF2738A, B and C, and their analogs produced by *Streptomyces* sp. *J. Antibiot.* **1994**, *47*, 1385–1394. [[CrossRef](#)]
39. Kivistik, P.A.; Kivisaar, M.; Hörak, R. Target Site Selection of *Pseudomonas putida* Transposon Tn4652. *J. Bacteriol.* **2007**, *189*, 3918. [[CrossRef](#)]

Publisher's Note: MDPI stays neutral with regard to jurisdictional claims in published maps and institutional affiliations.



© 2020 by the authors. Licensee MDPI, Basel, Switzerland. This article is an open access article distributed under the terms and conditions of the Creative Commons Attribution (CC BY) license (<http://creativecommons.org/licenses/by/4.0/>).